

## A FIRST-PRINCIPLES CALCULATION OF ELECTRONIC PROPERTIES OF LiNH<sub>2</sub> AND NaNH<sub>2</sub>

E. B. Kaizer, N. G. Kravchenko,  
and A. S. Poplavnoi

Band spectra, densities of states, total and deformation densities of  $\alpha$ -LiNH<sub>2</sub> and  $\alpha$ -NaNH<sub>2</sub> are calculated from the first principles using the density functional method in the all-electron approximation. The upper valence band is formed mostly by nitrogen *p*-states with a small admixture of metal states, the lower conduction bands are formed by the states of all atoms in  $\alpha$ -LiNH<sub>2</sub> and mainly by sodium and nitrogen states in  $\alpha$ -NaNH<sub>2</sub>. The bottom of the conduction band appears in both crystals in the center of the Brillouin zone.  $\alpha$ -LiNH<sub>2</sub> exhibits indirect-gap transitions at the absorption edge and three valence band extrema at a short distance of  $\sim 0.15$  eV from each other. The top of the valence band in  $\alpha$ -NaNH<sub>2</sub> appears in the center of the Brillouin zone with the competing maximum at the lateral point at a distance of  $\sim 0.06$  eV. The electron density distributions testify that polar covalent bonding occur inside the amide anion and ionic bonding occurs between the metal and the amide ion.

**DOI:** 10.1134/S002247661806001X

**Keywords:** density functional, electronic structure, electron density, chemical bonding, hydrogen storage, alkali metal amides.

### INTRODUCTION

The synthesis of alkali metal amides MNH<sub>2</sub> (M = Li, Na, K) was first reported in the early 19th century by Gay-Lussac with co-author (see the references to the early works e.g. in [1]). However, it is only recently that these compounds attracted increased interest as the most promising materials for the hydrogen storage and transport [2-4] due to high gravimetric density of hydrogen in these compounds. The studies concerning hydrogenation and dehydrogenation reactions involving alkali metal amides and imides (MNH<sub>2</sub>), the structure of these compounds and reaction products, and their physicochemical properties were reviewed in [2-4].

It is a well known fact that studying hydrogen containing compounds, including metal hydrides, with the method of X-ray structural analysis is hindered due to low resolution of hydrogen. A set of commonly used methods include powder neutron diffraction, synchrotron techniques, NMR spectroscopy in the presence of disorder structures, etc. First principles methods used to model the structures by optimizing their geometry also play an important role.

The crystal structure of  $\alpha$ -LiNH<sub>2</sub> was first determined using X-ray diffraction in 1951 [5]. Lithium amide at room temperature was found to form crystals of the tetragonal family with the space group 82 ( $S_4^2$ ) and eight formula units in the

---

Kemerovo State University, Russia; katerina.star@bk.ru. Translated from *Zhurnal Strukturnoi Khimii*, Vol. 59, No. 5, pp. 1301-1307, July-August, 2018. Original article submitted December 12, 2017.

unit cell. However, the obtained data raised doubts because of small minimal distance between the nitrogen and hydrogen atoms. Therefore, the structure was refined in [6] using high-resolution powder neutron diffraction. Of great interest are the studies concerning high-pressure phases of lithium amide.  $\alpha\text{-LiNH}_2 \rightarrow \beta\text{-LiNH}_2$  phase transition was established in [7] at a pressure of 12.5 GPa. However, the structure of the new phase was not determined. The structure of  $\beta\text{-LiNH}_2$  was determined by synchrotron X-ray diffraction measurements to be monoclinic, space group 4 ( $C_2^2$ ) [8].

IR spectroscopy and X-ray diffraction methods were used in [9] to detect a new intermediate phase, group 15 ( $C_{2h}^6$ ), with eight formula units in the unit cell at a pressure of 12.7 GPa and room temperature. It was also found that the final transition from the new intermediate to the  $\beta$ -phase occurs at 15.1 GPa.

Theoretical calculations predict numerous high-pressure phases [10, 11]. Besides experimentally determined phases [7-9], two more stable high-pressure phases are predicted:  $\beta\text{-LiNH}_2$  (orthorhombic,  $\text{NaNH}_2$ -type, group 70 ( $D_{2h}^{24}$ )) and  $\gamma\text{-LiNH}_2$  (orthorhombic, group 18 ( $D_2^3$ )). According to calculations, the ground-state phase of  $\alpha\text{-LiNH}_2$  is stable up to the pressure of 4.6 GPa [10] (6 GPa [11]) associated with the transition to the  $\beta\text{-LiNH}_2$  phase. The transition to the  $\gamma$ -phase occurs at  $\sim$ 11 GPa.

Sodium amide ( $\text{NaNH}_2$ ) belongs to the group of alkali amides. In spite of a relatively low hydrogen content (5.2 wt.%), it demonstrated promising opportunities for hydrogen storage. However, in contrast to lithium amide, it has been little studied. Its structure was experimentally determined in [12] for  $\text{NaND}_2$ . Replacing hydrogen with deuterium in experimental studies increases the accuracy of determining atomic positions. However, many physicochemical properties of  $\text{NaNH}_2$  and  $\text{NaND}_2$  are different, since the mass of D is twice as large as the mass of H. It was reported in [12] that  $\text{NaND}_2$  crystals exhibit the orthorhombic lattice, group 70 ( $D_{2h}^{24}$ ). IR and Raman spectroscopy studies of  $\text{NaNH}_2$  under pressure [13] revealed significant changes in IR and Raman frequencies at about 0.9 GPa and 2.0 GPa to indicate phase transitions. The structures of high-pressure phases were established theoretically in [14]. The ground-state  $\alpha\text{-NaNH}_2$  was found to transform into an orthorhombic  $\beta\text{-NaNH}_2$  (space group 18 ( $D_2^3$ )) at 2.2 GPa and then into a monoclinic  $\gamma\text{-NaNH}_2$  (space group 15 ( $C_{2h}^6$ )) at 9.4 GPa.

Besides structural studies, understanding fundamental properties of alkali metal amides requires studying their electronic structure, chemical bonding, and elastic properties. Usually, these are theoretical studies [1, 6, 8, 10, 11, 14-16] concerning mainly lithium amide. The early works [6, 15, 16] reported studying electronic structure of tetragonal  $\text{LiNH}_2$  with first principles density functional calculations using linearized plane waves [6], pseudopotential [15], and projector-augmented plane waves [16]. It was established that chemical bonding is ionic between  $\text{Li}^+$  and  $(\text{NH}_2)^-$  ions and covalent inside the  $(\text{NH}_2)^-$  anion. Accordingly, the valence band is formed mainly by the states of the  $(\text{NH}_2)^-$  anion, and the conduction band is formed by the states of the metal. The calculated band gaps are 3.48 eV [6], 3.2 eV [15]. No exact values are given in [16], and it is reported that  $E_g \sim 3$  eV. The band edge structure is not discussed in these works and cannot be determined from the reported densities of states. High-pressure phases of lithium amide were studied in [8, 10, 11] with the density functional method to obtain the density states of  $\alpha$ - and  $\beta\text{-LiNH}_2$  [8], phonon density of states and electron density distributions of  $\alpha$ -,  $\beta$ -,  $\gamma\text{-LiNH}_2$  [10], and densities of states of these three phases [11].

Electronic and vibrational properties of sodium amide were studied in [1, 14]. The density functional theory was used in [14] to calculate the maps of electron density, electron and phonon state densities of  $\alpha$ -,  $\beta$ -,  $\gamma\text{-NaNH}_2$  when studying high-pressure phases of this compound. As mentioned in [1], electronic, elastic, and optical properties of alkali metal amides are still poorly studied, with the exception of lithium amide. Besides, there are no comparative studies to share a common methodology. The work reported the first principles calculations of electronic structure, elastic and optical constants for a group of  $\text{LiNH}_2$ ,  $\text{NaNH}_2$ ,  $\text{KNH}_2$ , and  $\text{RbNH}_2$  compounds and discussed some dependences of their physical properties.

The present work reports precise calculations of structure constants, band spectra, density of states, and total and deformation density distributions for the tetragonal  $\text{LiNH}_2$  and the orthorhombic  $\text{NaNH}_2$ .

## CALCULATION METHOD AND GEOMETRY OPTIMIZATION

The structural parameters, band spectra, and electron density distributions were calculated with the Crystal14 software [17, 18] within the density functional method and the full-electron approach in the LCAO approximation. The calculations implied the B3LYP hybrid exchange-correlation potential which combines the Becke exchange functional and the LYP nonlocal correlation potential along with the Hartree-Fock exchange component. The integration in the direct space was carried out using a radial (75,974) grid with 75 radial points and the maximum of 974 corner points in the region of chemical bonding. The integration over the Brillouin zone in the reciprocal space was performed using a  $16 \times 16 \times 16$  Monkhorst-Pack grid. Contracted Gaussian orbitals were used as basis functions [19].

The above method was initially used to calculate the structural parameters of  $\text{LiNH}_2$  and  $\text{NaNH}_2$ . According to our calculations and to those reported in [1], different exchange-correlation potentials provide substantially different values of structural parameters, so that the discrepancy may exceed 10% in the compounds with complex unit cells, as is the case of  $\text{NaNH}_2$  ( $Z = 16$ ) [1]. Also, structural parameters depend substantially on the basis chosen. We performed 48 calculations to determine the optimal basis for sodium amide. The lowest total energies and the best agreement with experimental lattice constants were obtained by combining the basis sets for Li, Na [20], N [21], and H [22]. The structural parameters obtained with these calculations are presented in Table 1.

**TABLE 1.** Structural Characteristics of  $\text{LiNH}_2$  and  $\text{NaNH}_2$

Compound	Space group, number of formula units $Z$	Lattice constants, Å	Coordinates of nonequivalent atoms	$d_{\text{M-N}}$ , $d_{\text{N-H}}$ , Å, $\angle(\text{H}-\text{N}-\text{H})$ , deg
$\alpha\text{-LiNH}_2$ [ 6 ] (exp.)	No. 82 ( $S_4^2$ ) tetragonal $Z = 8$	$a = 5.034$ , $c = 10.255$	Li1 (0.0, 0.0, 0.0)	2.0933
			Li2 (0.0, 0.5, 0.0042)	2.0779
			Li3 (0.0, 0.0, 0.25)	2.1919
			N (0.22860, 0.2499, 0.1158)	0.9868
			H1 (0.24290, 0.1285, 0.1910)	0.9420
			H2 (0.38400, 0.3512, 0.1278)	99.97°
$\alpha\text{-LiNH}_2$ [ our calculations]	No. 82 ( $S_4^2$ ) tetragonal $Z = 8$	$a = 5.045$ , $c = 10.378$ , $\delta_a = 0.1\%$ $\delta_c = 1.0\%$	Li1 (0.0, 0.0, 0.0)	2.0682
			Li2 (0.0, 0.5, 0.0044)	2.2214
			Li3 (0.0, 0.5, 0.25)	2.2256
			N (0.2278, 0.2455, 0.1149)	1.0244
			H1 (0.2312, 0.1159, 0.1912)	1.0114
			H2 (0.4061, 0.3407, 0.1247)	101.946°
$\alpha\text{-NaNH}_2$ [ 12 ] (exp.)	No. 70 ( $D_{2h}^{24}$ ) orthorhombic $Z = 16$	$a = 8.949$ , $b = 10.456$ , $c = 8.061$	Na (0.125, 0.125, 0.27020)	2.4371
			N (0.36150, 0.125, 0.125)	2.4936
			H (0.43000, 0.06200, 0.02800)	1.2851
				129.11°
$\alpha\text{-NaNH}_2$ [ our calculations]	No. 70 ( $D_{2h}^{24}$ ) orthorhombic $Z = 16$	$a = 8.748$ , $b = 10.451$ , $c = 8.138$ , $\delta_a = 2.4\%$ , $\delta_b = 0.0\%$ , $\delta_c = 0.8\%$	Na (0.125, 0.998, 0.125)	2.4567
			N (0.125, 0.125, 0.989)	2.4137
			H (0.0816, 0.1915, 0.8118)	1.0310
				100.4°

## BAND STRUCTURE AND DENSITIES OF STATES

The band structure was calculated along the symmetry directions of the Brillouin zones: M–Γ–X–P–N for  $\alpha$ -LiNH<sub>2</sub> and Y–Γ–Z–T–L for  $\alpha$ -NaNH<sub>2</sub> (Fig. 1a). The calculated band spectra are shown in Fig. 1b. The bottom of the conduction

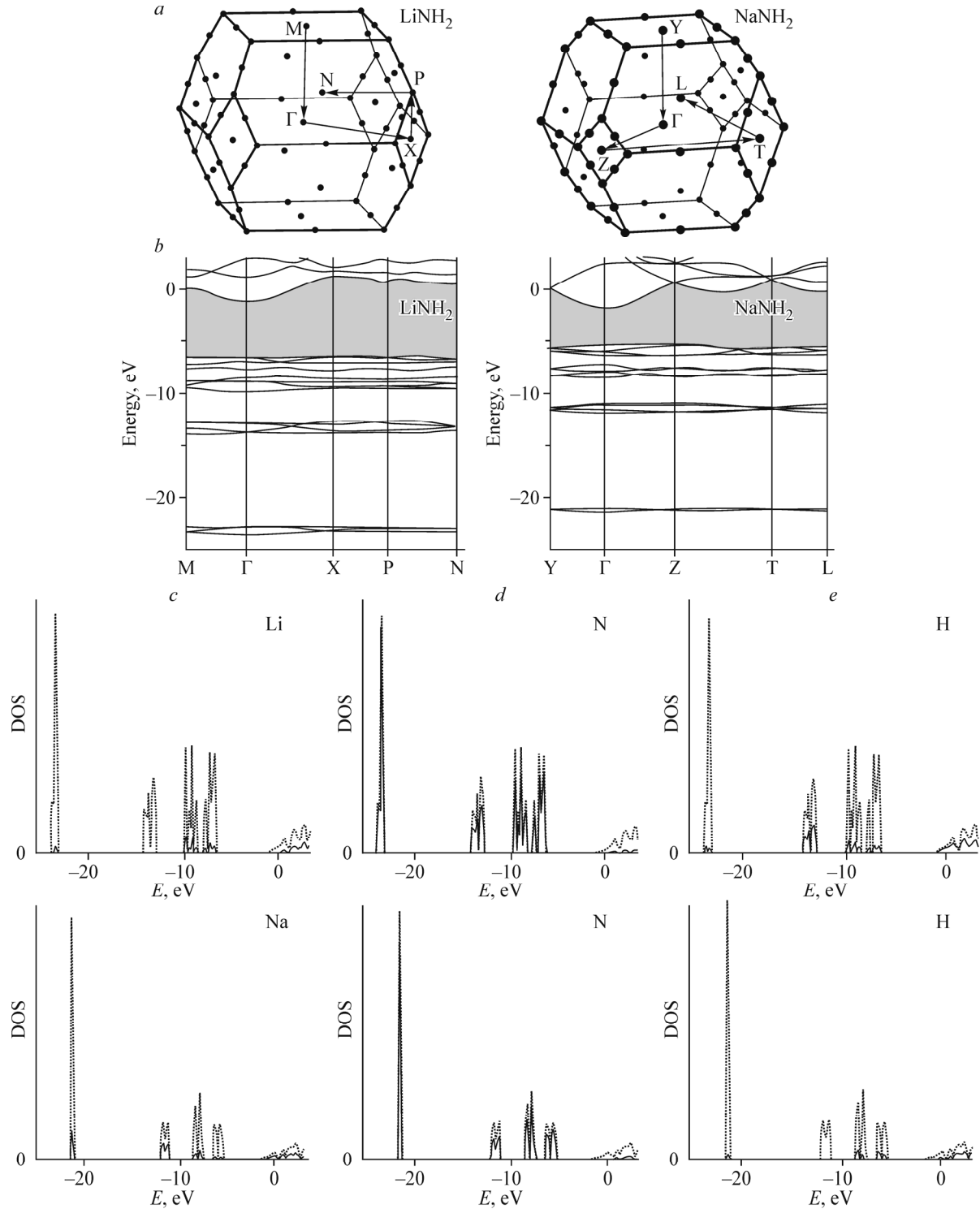


**Fig. 1.** Brillouin zones (*a*), electronic structure (*b*), total (gray line) and partial (bold line) density of states for  $\alpha$ -LiNH<sub>2</sub> (top) and  $\alpha$ -NaNH<sub>2</sub> (bottom) (*c*–*e*).

band appears in both crystals in the center of the Brillouin zone (point  $\Gamma$ ). The top of the valence band (VB) in  $\alpha\text{-LiNH}_2$  appears at the point X at a distance of  $\sim 0.15$  eV from the nearest maxima at the points P and M to indicate indirect-gap transitions at the absorption edge. The top of the VB in the  $\alpha\text{-NaNH}_2$  crystal appears at the point  $\Gamma$ , which is  $\sim 0.06$  eV higher than the nearest maximum at the point Z to indicate direct-gap transitions.

The VB is formed in both crystals by sixteen zones divided into four bunches, four zones in each bunch. In the absolute energy scale, the VB appears in the range from  $-24$  eV to  $-7$  eV in  $\alpha\text{-LiNH}_2$  and from  $-21$  eV to  $-5$  eV in  $\alpha\text{-NaNH}_2$ . The spectral composition of the energy band bunches was determined using total and partial densities of states (Fig. 1c-e). As can be seen, cation states in both crystals provide some small contribution to the two upper VB bunches, so that the VB is composed mainly by the anion states. The lower bunch is formed mainly by N 2s and H 1s states. The next bunch is formed by N 2p and H 1s states. The two upper filled VB bunches are formed mainly by N p-electrons and, as already mentioned, include some small contribution of cation electronic states. The first two unoccupied orbitals are formed by all atoms in  $\alpha\text{-LiNH}_2$  and mainly by sodium and nitrogen atoms in  $\alpha\text{-NaNH}_2$ .

Table 2 presents some main characteristics calculated for the band spectra of  $\alpha\text{-LiNH}_2$  and  $\alpha\text{-NaNH}_2$  crystals: band gaps  $E_g$ , valence bands  $\Delta E_v$ , and the widths of valence band bunches  $\Delta E_1\text{--}\Delta E_4$ , starting from top down.

The direct band gap  $E_g$  ( $\Gamma\text{--}\Gamma$ ) in  $\alpha\text{-LiNH}_2$  is  $5.47$  eV, which is  $0.16$  eV larger than the indirect gap. The indirect band gaps calculated in earlier works for  $\alpha\text{-LiNH}_2$  were  $3.48$  eV [6],  $3.2$  eV [15],  $\sim 3$  eV [16]. The later work [1] reported  $E_g = 4.95$  eV, which is closer to our data. It was mentioned in this work that the numerical value  $E_g$  depends on the specific density functional method used, so experimental data are required to solve the problem. The band structure for  $\alpha\text{-NaNH}_2$  was calculated earlier only in [1] to give  $E_g = 3.55$  eV, which is virtually coinciding with our result.

The widths of the bunches reflect the hybridization degree between the atomic states to form the bunches. As can be seen from Table 2, all four VB bunches, as well as the total valence bands, are larger in  $\alpha\text{-LiNH}_2$  as compared to  $\alpha\text{-NaNH}_2$ . Some weaker hybridization in  $\alpha\text{-NaNH}_2$  can be explained by larger distances  $d_{M\text{-}N}$  and  $d_{N\text{-}H}$  between immediate neighbors in  $\alpha\text{-NaNH}_2$  as compared to  $\alpha\text{-LiNH}_2$  (Table 1).

## TOTAL AND DEFORMATION ELECTRON DENSITIES

To study chemical bonding in the  $\alpha\text{-LiNH}_2$  and  $\alpha\text{-NaNH}_2$  crystals in detail, we computed and plotted the total  $\rho(\mathbf{r})$  and deformation  $\Delta\rho(\mathbf{r})$  density distributions in various planes. Fig. 2 shows density distributions for lithium amide; solid and dashed isolines show positive and negative values of the electron density, respectively. Distributions obtained for sodium amide are all topologically similar, the differences are only in their absolute values (discussed below).

The maps of total electron density for both crystals exhibit a closed molecular contour around the amide anion, with the density values of  $0.25$  e/bohr<sup>3</sup> and  $0.3$  e/bohr<sup>3</sup> in  $\text{LiNH}_2$  and  $\text{NaNH}_2$ , respectively. The deformation densities demonstrate maxima on the line of the N-H bond near the nitrogen and hydrogen atoms. All this testifies polar covalent bonding appearing in the amide anion.

As far as the bonding between the cation and the anion complex, there are contours of the total electron density around these structures. However, the magnitude of crystal density is negligible ( $0.02$  e/bohr<sup>3</sup> in both crystals), and the deformation density is negative on the cation and positive on the amide ion to indicate predominantly ionic bonding.

Consider the electron density distribution in the cation plane in  $\text{LiNH}_2$ . The regions of the total and deformation densities between lithium atoms demonstrate small maxima with the magnitude of the total electron density of  $0.05$  e/bohr<sup>3</sup>

**TABLE 2.** Main Characteristics of  $\text{LiNH}_2$  and  $\text{NaNH}_2$  Band Spectra

Crystal	$E_g$ , eV	$\Delta E_v$ , eV	$\Delta E_1$ , eV	$\Delta E_2$ , eV	$\Delta E_3$ , eV	$\Delta E_4$ , eV
$\text{LiNH}_2$	(X- $\Gamma$ ) $5.31$	$17.14$	$1.38$	$1.47$	$1.25$	$0.62$
$\text{NaNH}_2$	( $\Gamma\text{--}\Gamma$ ) $3.54$	$16.06$	$1.08$	$1.12$	$0.94$	$0.33$

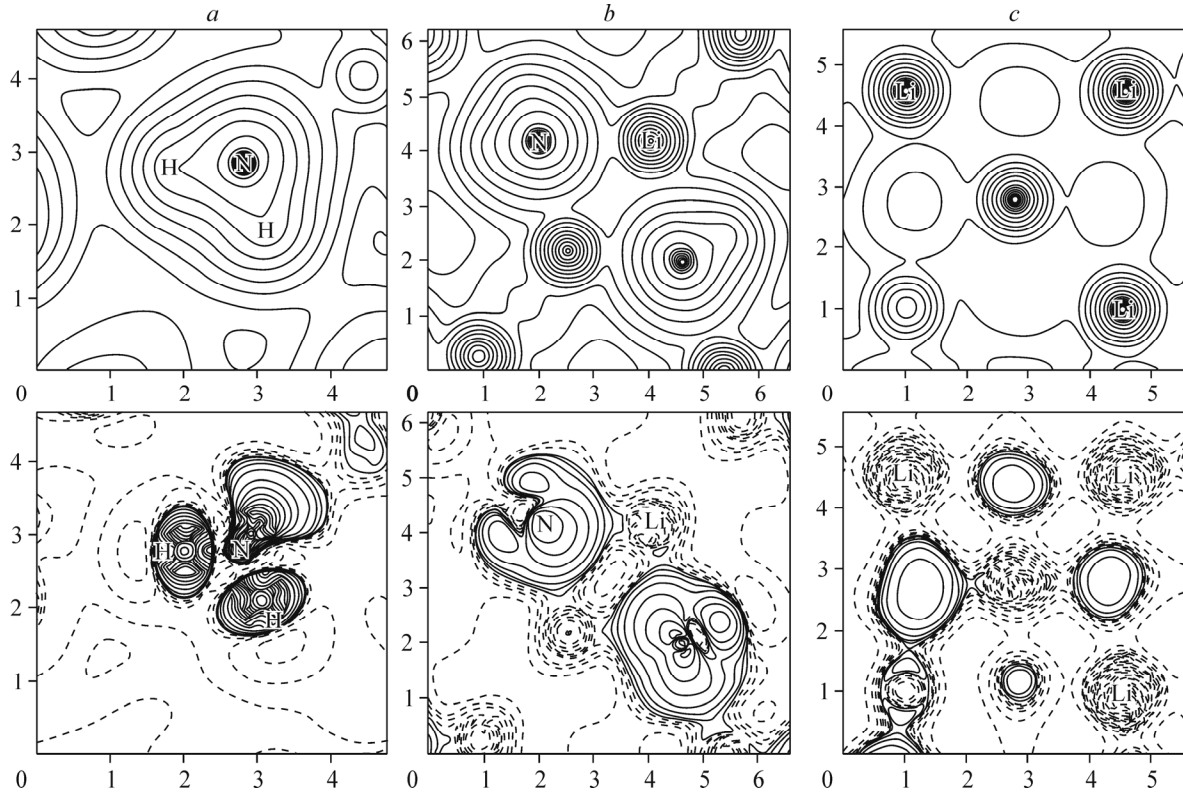


**Fig. 2.** Total crystalline (top) and deformation (bottom) density distributions in  $\text{LiNH}_2$  imaged in the amide anion plane (a),  $\text{Li}-\text{N}-\text{Li}$  plane (b), and in the cation plane (c).

and  $0.01 \text{ e}/\text{bohr}^3$ . As follows from the detailed analysis of the crystalline structure, these maxima are due to the presence of nitrogen atoms directly above or below these positions. Similar maxima with vanishing magnitudes are also observed in sodium amide.

## CONCLUSIONS

A common problem of determining the exact coordinates of hydrogen atoms in crystal structures can be solved by theoretical methods using structure optimizations. This task requires up to date density functional methods and carefully chosen optimal basis functions, which is especially true for the crystals with a complex unit cell. We performed first principles full-electron calculations of the structural parameters of  $\alpha$ - $\text{LiNH}_2$  and  $\alpha$ - $\text{NaNH}_2$  crystals using the Crystal14 software to determine their lattice parameters with a maximum error of 2.4% for one of the parameters of  $\alpha$ - $\text{NaNH}_2$  ( $Z = 16$ ). Calculated band structures, densities of states, and electron density distributions in  $\alpha$ - $\text{LiNH}_2$  and  $\alpha$ - $\text{NaNH}_2$  turned out to be qualitatively similar, in spite of the fact that they belong to different crystal families (tetragonal ( $S_4^2$ ) and orthorhombic ( $D_{2h}^{24}$ ), respectively). This is due to the similarity of their crystal structures, in particular, the ( $D_{2h}^{24}$ ) space group corresponds to the  $\beta$ - $\text{LiNH}_2$  high-pressure phase. The quantitative differences in the band structures were manifested as different arrangements of the band edges and different structures of the absorption edges: direct gap transition in  $\alpha$ - $\text{LiNH}_2$  and indirect gap transition in  $\alpha$ - $\text{NaNH}_2$ . The distances  $d_{\text{M-N}}$  and  $d_{\text{N-H}}$  between the nearest neighbors turned out to be larger in  $\alpha$ - $\text{LiNH}_2$  than in  $\alpha$ - $\text{NaNH}_2$  to indicate weaker hybridization of atomic states. A known conclusion that chemical bonding is polar covalent in the amide anion and is ionic between the metal and the amide ion in  $\alpha$ - $\text{LiNH}_2$  is shown to be true also for  $\alpha$ - $\text{NaNH}_2$ .

## REFERENCES

1. K. R Babu and G.Vaitheeswaran. *J. Phys.: Condens. Matter.*, **2014**, *26*, 235503.
2. B. P. Tarasov, M. V. Lototskii, and V. A. Yartys. *Rus. J. Gen. Chem.*, **2006**, *L(6)*, 34.
3. V. M. Azhazha, M. A. Tikhonovsky, A. G. Shepelev, Yu. P. Kurilo, T. A. Ponomarenko, and D. V. Vinogradov. *Probl. At. Sci. Technol.*, **2006**, *15*(1), 145.
4. B. Sakintuna, F. Lamari-Darkrim, and M. Hirscher. *Int. J. Hydrogen Energy*, **2007**, *32*, 1121.
5. R. Juza and K. Opp. *Z. Anorg. Allg. Chem.*, **1951**, *266*, 313.
6. J. B. Yang, X. D. Zhou, W. J. James, and W. B. Yelon. *Appl. Phys.*, **2006**, *88*, 041914.
7. R. S. Chellappa, D. Chandra, M. Somayazulu, S. A. Gramsch, and R. J. Hemley. *J. Phys. Chem. B*, **2007**, *111*, 10785.
8. X. Huang, D. Li, F. Li, X. Jin, S. Jiang, W. Li, X. Yang, Q. Zhou, B. Zou, Q. Cui, B. Liu, and T. Cui. *J. Phys. Chem. C*, **2012**, *116*, 9744.
9. H. Yamawaki, H. Fujihisa, Y. Gotoh, and S. Nakano. *J. Phys. Chem. B*, **2014**, *118*, 9991.
10. Y. Zhong, H. Zhou, Ch. Hu, D. Wang, and G. Rao. *J. All. Comp.*, **2012**, *544*, 129.
11. D. L. V. K. Prasad, N. W. Ashcroft, and R. Hoffmann. *J. Phys. Chem. A*, **2012**, *116*, 10027.
12. M. Nagib, H. Kistrup, and H. Jacobs. *Atomkernenergie*, **1975**, *26*, 87.
13. A. Liu and Y. Song. *J. Phys. Chem. B*, **2011**, *115*, 7.
14. Y. Zhong, H. Zhou, C. Hu, D. Wang, and A. R. Oganov. *J. Phys. Chem. C*, **2012**, *116*, 8387.
15. K. Miwa, N. Ohba, and S. Towata. *Phys. Rev. B*, **2005**, *71*, 195109.
16. J. F. Herbst and L. G. Hector Jr. *Phys. Rev. B*, **2005**, *72*, 125120.
17. R. Dovesi, V. R. Saunders, C. Roetti, and R. Orlando. CRYSTAL14 User's Manual, **2009**.
18. R. Dovesi, R. Orlando, B. Civalleri, C. Roetti, V. R. Saunders, and C. M. Zicovich-Wilson. *Zeit. Kristallogr.*, **2005**, *220*(5-6), 571.
19. <http://www.crystal.unito.it/basis-sets.php>.
20. M. F. Peintinger, D. V. Oliveira, and T. Bredow. *J. Comput. Chem.*, **2013**, *34*(6), 451.
21. R. Dovesi, M. Causa, R. Orlando, and C. Roetti. *J. Chem. Phys.*, **1990**, *92*, 7402.
22. R. Dovesi, E. Ermondi, E. Ferrero, C. Pisani, and C. Roetti. *Phys. Rev.*, **1983**, *B29*, 3591-3600.